

## **Ti(III)APO-5 materials as selective catalysts for the allylic oxidation of cyclohexene: Effect of Ti source and Ti content**

*Almudena Alfayate, Carlos Márquez-Álvarez, Marisol Grande-Casas, Manuel Sánchez-Sánchez and Joaquín Pérez-Pariente\**

Instituto de Catálisis y Petroleoquímica, ICP-CSIC, C/ Marie Curie 2, 28049 Madrid, Spain

\*To whom correspondence should be addressed:

Dr. Joaquín Pérez-Pariente. E-mail address: [jperez@icp.csic.es](mailto:jperez@icp.csic.es)

Telephone: +34-915854784. Fax: +34-915854760.

### ABSTRACT.

Different TAPO-5 materials, prepared from Ti(III) chloride, have been tested as catalysts in the oxidation of cyclohexene with hydrogen peroxide under anhydrous conditions. Solid  $\text{TiCl}_3$  was shown to render better synthesis reproducibility and higher catalytic activity of the resultant materials compared to  $\text{TiCl}_3$  aqueous solution. The synthesis of these materials was carried out under  $\text{N}_2$  atmosphere to preserve the initial oxidation state of Ti during the crystallization process. As a consequence, the so-called Ti(III)APO-5 materials have Ti environments different to those found in conventional TAPO-5 (Ti(IV)APO-5). Indeed, their catalytic activity in the oxidation of cyclohexene markedly overcomes that of the Ti(IV)APO-5 at any Ti content and after any reaction time. Turnover number (TON) of Ti(III)APO-5 samples exponentially increases as Ti content decreases, the Ti-poorer sample (Ti/(Ti+Al+P) molar ratio of 0.003) reaching

TON values higher than 200 after 6 h of reaction at 343 K and higher than 550 after 24 h. The interest of Ti(III)APO-5 catalysts lies on their high selectivity to products formed through allylic oxidation of cyclohexene. The main product of this reaction, 2-cyclohexenyl hydroperoxide, was obtained with more than 80 % selectivity over Ti(III)APO-5 catalysts. This behavior is in contrast with the well-known strong tendency of the more active Ti-zeolites to epoxidize the double bond.

KEYWORDS.

TAPO-5, Ti(III)APO-5, cyclohexene oxidation, allylic oxidation, Ti(III) source, 2-cyclohexenyl hydroperoxide.

## **Introduction**

Since the discovery in the early eighties of the ability of TS-1 to catalyze the selective oxidation of organic compounds [1], the application of Ti-zeolites as heterogeneous catalysts for the oxidation of organic substrates under mild conditions has been the subject of a large number of studies [2-5]. The interest in this kind of zeolitic materials led to explore other potential Ti-containing materials, such as silica-based mesoporous ones, which would allow processing larger molecules [6-8]. However, in contrast to the continuous development of highly active Ti-zeolites and Ti-mesoporous materials, the attempts carried out with the related group of titanium-doped  $\text{AlPO}_4$ -based microporous zeotypes have failed to render interesting catalysts. In spite of the large number of the so-called TAPO materials with different structures that have been prepared [9-11], up to

date, their catalytic performance in those oxidation processes [12-15] has been shown poor compared to that of Ti-zeolites.

Several aspects that make TAPOs different to Ti-zeolites have to be considered in order to develop strategies to enhance their catalytic performance. First, both networks are inherently different in hydrophobic/hydrophilic terms, in such a way that the more hydrophilic  $\text{AlPO}_4$  framework favors the selective adsorption of the most polar molecules. The influence of hydrophobicity/hydrophilicity on the catalytic activity has been already made clear in Ti-zeolites by modifying the polarity of their frameworks or the reaction conditions [4, 15-18]. A second difference between TAPOs and Ti-zeolites is the Ti environment obtained by the isomorphous substitution of tetrahedral atoms in both materials. When Ti(IV) ions are introduced in zeolitic frameworks, they can only substitute isoelectronic Si(IV) atoms, necessarily leading to  $\text{Ti}(\text{OSi})_4$  environments. However, Ti(IV) replaces more likely P(V) atoms in an  $\text{AlPO}_4$  framework, generating  $\text{Ti}(\text{OAl})_4$  environments. Such environments are thought to inhibit the activity of Ti centers as deduced from the lower catalytic activity of Ti-zeolites containing aluminum compared with their Al-free analogues [4, 19]. Recently, Chiesa and co-workers [20-22] have reported some spectroscopic studies indicating that Ti(IV) in an  $\text{AlPO}_4$  material can also be incorporated by pairs, so that two Ti atoms replace a P(V) atom and its contiguous Al(III) generating Ti-O-Ti units, just like Si(IV) can do in the case of SAPO materials [23, 24]. Moreover, though isolated titanium centers in P(V) positions and/or Ti-O-Ti pairs are found in the material, titanium atoms in aluminum sites have been proven to play the most important role for redox catalytic activity [22].

Recently, we have presented some innovative strategies in TAPO-5 synthesis [25, 26], which take advantage of the higher versatility of  $\text{AlPO}_4$  frameworks compared to zeolite ones to incorporate heteroatom ions with different charges. Such versatility would, in

principle, allow to change the Ti environment within the aluminophosphate framework by means of its incorporation as Ti(III). This cation would occupy preferably Al(III) sites in order to maintain the charge balance of the framework, and would give rise to Ti(OP)<sub>4</sub> environments. In addition, the presence of Ti-O-Ti pairs would be prevented since replacing contiguous P(V) and Al(III) by two Ti(III) ions would entail an excessive negative charge in the framework, hardly compensated by a mono-protonable amine, which is the most common structure directing agent in AlPOs.

We have reported elsewhere that this approach indeed generates TAPO-5 catalysts that are more active than the conventional ones, being able to oxidize cyclohexene at a rate of the same order as large-pore Ti-beta [27] under suitable conditions. This work extends the study of TAPO-5 materials prepared from gels containing Ti(III) ions, here called Ti(III)APO-5, as catalysts in the cyclohexene oxidation with H<sub>2</sub>O<sub>2</sub> under anhydrous conditions. The influence that Ti content in Ti(III)APO-5 materials has on the intrinsic activity of Ti centers has been also investigated, discussed, and critically compared with the conventional TAPO-5 catalysts prepared using Ti(IV) sources.

## **2. Experimental**

### *2.1. Catalysts preparation*

Ti(III)APO-5 samples were prepared with different titanium content by hydrothermal treatment using titanium trichloride as Ti(III) source [25, 26], in one of these two formulations: (i) as TiCl<sub>3</sub> (~10 wt.%) in HCl (20-30 wt.%) aqueous solution (supplied by Aldrich with the exact composition), and (ii) TiCl<sub>3</sub> powder (Aldrich). The general gel composition was (1-x) Al : 1.0 P : x Ti(III) : m MCHA : 25 H<sub>2</sub>O : n HCl for the former TiCl<sub>3</sub> source, where x denotes the Ti/P molar ratio, n is the HCl/P molar ratio

resultant after its inevitable addition with  $\text{TiCl}_3$  in hydrochloric acid solution, MCHA refers to N-methyldicyclohexylamine and  $m$  designates the MCHA/P molar ratio, which was varied to compensate the changes of pH introduced by the HCl added, so that the pH value of the gel was forced to be in the range 6.5-7.0. When the  $\text{TiCl}_3$  powder was used, the gel composition was simplified to  $(1-x) \text{ Al} : 1.0 \text{ P} : x \text{ Ti(III)} : 0.8 \text{ MCHA} : 25 \text{ H}_2\text{O}$  having pH values in the same range. Both the preparation of the gel and the following autoclaves sealing were carried out under inert atmosphere, in a glove bag filled with nitrogen. The  $\text{TiCl}_3$  source was added over an aqueous solution of phosphoric acid (85 wt. %, Sigma) in deionized water, which turns into purple color. Next,  $\text{Al(OH)}_3 \cdot x\text{H}_2\text{O}$  (Sigma-Aldrich) was added over the solution and the resultant suspension was vigorously stirred for *ca.* 10 min, followed by the dropwise addition of N-methyldicyclohexylamine (MCHA). This amine was selected as structure directing agent (SDA) because of its high specificity to AFI-structured  $\text{AlPO}_4$ -based materials [28]. In particular, this specificity has already been proven for  $\text{AlPO}_4$  materials doped with the same heteroatom, Sn, in two different oxidation states [29]. The resultant gel was stirred for 1 h before transferring it into Teflon-lined stainless steel autoclaves for the hydrothermal treatment at 448 K under autogeneous pressure. The obtained purple solids, whose color indicated that at least part of the Ti present in the solid maintains its oxidation state 3+ after the crystallization process, were recovered by filtration and washed with deionized water. After drying under ambient atmosphere, the solids became yellowish white, suggesting that Ti(III) was oxidized to the most stable titanium oxidation state, Ti(IV).

Conventional Ti(IV)APO-5 catalysts were prepared strictly following the procedure described elsewhere [30], with the molar gel composition  $1.0 \text{ Al} : 1.0 \text{ P} : x \text{ Ti(IV)} : 0.5 \text{ TPAOH} : 20 \text{ H}_2\text{O}$ , using titanium isopropoxide (Aldrich) as Ti(IV) source.

The samples prepared with Ti(III) sources will be named as Ti(III)APO-5, while Ti(IV)APO-5 will denote the conventional samples prepared with the Ti(IV). The general term TAPO-5 will be used to refer to both Ti(III)APO-5 and Ti(IV)APO-5 materials. The nomenclature used for every particular solid will be as follows: the oxidation state of titanium source, followed by a letter only in the case of Ti(III)APO-5 samples to indicate the type of TiCl<sub>3</sub> source used ('p' for powder and 's' for solution), next a number that will indicate the titanium/phosphorous percent molar ratio in the gel (x 100 times) and finally the crystallization time will be indicated by the number of hours (h) or days (d). As an example, Ti(III)p-1-4h will then denote the sample prepared with TiCl<sub>3</sub> powder, with a titanium content in the gel  $x = 0.01$  and after 4 h of crystallization.

Prior to catalytic tests, all TAPO-5 samples were calcined, in order to eliminate the SDA molecules. The solid samples were heated under a N<sub>2</sub> flow of 100 mL·min<sup>-1</sup> from room temperature to 823 K (at a heating rate of 3 K·min<sup>-1</sup>) and kept at this temperature for 1 h. Then they were maintained under an air flow of 100 mL·min<sup>-1</sup> at 823 K for 5 h. Complete removal of the organic molecules was certified by thermogravimetric analysis.

## 2.2. Characterization techniques

Nature and purity of crystalline phases were studied by powder X-ray diffraction (PXRD) using a PANalytical X'Pert Pro diffractometer (Cu K $\alpha$  radiation). Diffuse reflectance UV-visible (DRUV) spectra were recorded with a Cary 5000 Varian spectrophotometer equipped with an integrating sphere using the synthetic polymer Spectralon as reference. The spectra were corrected applying the Kubelka-Munk

function. The chemical composition of the solids was determined by inductively coupled plasma (ICP-OES) spectrometry with an ICP Winlab Optima 3300 DV Perkin-Elmer spectrometer. Scanning electron microscopy (SEM) micrographs were taken in a FEI Nova NANOSEM microscope with a vCD detector. Nitrogen adsorption/desorption isotherms were measured at 77 K in a Micromeritics ASAP 2010 equipment. Calcined samples were previously degassed at 623 K for 16 h. Surface areas were estimated by applying the BET method, and micropore volume was obtained by application of the t-plot method to the N<sub>2</sub> adsorption data.

### *2.3. Catalytic experiments*

Catalysts were tested in the oxidation of cyclohexene with H<sub>2</sub>O<sub>2</sub> under anhydrous conditions as described elsewhere [27]. These conditions were reached after removing almost all the water that accompanies the commercial 30 wt. % H<sub>2</sub>O<sub>2</sub> aqueous solution. Water was removed by Soxhlet extraction of solutions prepared dissolving the 30 wt. % H<sub>2</sub>O<sub>2</sub> solution in acetonitrile. The reactions were carried out in batch mode using a round bottom flask equipped with a magnetic stirrer, a thermometer and a covered reflux condenser provided with a drying tube on top. The latter was used in order to avoid the condensation of ambient humidity inside the condenser caused by the low temperature of water circulating through it. The coolant water temperature was controlled at 278 K to prevent any evaporation of the chemicals during the reaction. Calcined catalysts were activated overnight inside the reaction system at 433 K under a flow of N<sub>2</sub> to remove any water adsorbed into the catalyst channels. Under the reaction conditions used, mass balance was *ca.* 98 % after 30 h of reaction.

In a typical experiment, 3.0 g of cyclohexene, the corresponding amount of H<sub>2</sub>O<sub>2</sub> in CH<sub>3</sub>CN solution (previously submitted to Soxhlet extraction of water) and additional acetonitrile, if necessary, were mixed to reach a molar ratio CH<sub>3</sub>CN : H<sub>2</sub>O<sub>2</sub> : cyclohexene of 20 : 0.55 : 1. Toluene was added as internal standard. This solution was poured into the flask containing the activated catalyst (cyclohexene/ catalyst weight ratio of 10). The reaction mixture was heated up to 343 K under continuous stirring. The reaction progress was followed by taking different aliquots under stirring. The time zero aliquot was taken when the setpoint temperature was reached in the mixture. Products were separated and analyzed by gas chromatography in a Varian CP-3380 gas chromatograph equipped with a capillary column (dimethylpolysiloxane) with length of 15 m, i.d. of 0.25 mm and thickness of 1 μm, and a flame ionization detector (FID). Products were identified by mass spectrometry, <sup>1</sup>H and <sup>13</sup>C NMR and infrared spectroscopies, as described elsewhere [27]. Conversions were calculated from the yields of the resultant products. In order to study the possible leaching of Ti from the heterogeneous catalysts during the reaction, all the final reaction mixtures were filtered and analyzed by total X-ray fluorescence. No traces of titanium were found in these solutions for any of the catalysts tested (detection limit of the technique was below 0.1 ppm). A blank experiment was performed under the same reaction conditions resulting in a total conversion lower than 5 % after 30 h.

### **3. Results and discussion**

#### *3.1. Catalysts characterization*

Table 1 summarizes the composition of the gels and the as-prepared catalysts. Titanium incorporation was less effective when Ti(IV) source was used, the titanium content in



the solid being lower than in the starting gel. In contrast, the titanium content of catalysts obtained with Ti(III) sources was in all cases equal to or higher than that of the corresponding gel. For this reason, later discussions about characterization and catalytic activity results will be done comparing Ti(III)APO-5 and Ti(IV)APO-5 samples with similar titanium content in the solid recovered, instead of those prepared with the same Ti content in the synthesis gel. Hence Ti(III)p-0.5-4h will be compared with Ti(IV)-1-8d and Ti(III)p-1-4h with Ti(IV)-2-8d.

Powder X-ray diffraction patterns of as-prepared samples are shown in Figure 1. All the materials show the typical pattern of pure AFI phase and no signals of impurities appear in the diffractograms. After calcination, all samples kept the pure AFI phase. It is noticeable that at high content of titanium longer crystallization times were necessary to achieve crystallinities similar to those obtained at lower content of this heteroatom.

**Table 1**

Ti, Al and P content of the synthesis gels and corresponding values determined by ICP-OES for as-prepared Ti(III)APO-5 and Ti(IV)APO-5 samples.

Sample	Gel composition <sup>a</sup>			Solid composition <sup>a</sup>		
	Ti	Al	P	Ti	Al	P
Ti(III)p-0.5-4h	0.005	0.995	1.00	0.006	1.012	0.982
Ti(III)p-1-4h	0.01	0.99	1.00	0.009	1.011	0.980
Ti(III)p-2-4h	0.02	0.98	1.00	0.034	1.025	0.941
Ti(III)p-4-4h	0.04	0.96	1.00	0.069	1.026	0.905
Ti(III)p-4-18h	0.04	0.96	1.00	0.065	0.928	1.007
Ti(III)s-4-18h	0.04	0.96	1.00	0.062	0.988	0.950
Ti(IV)-1-8d	0.01	1.00	1.00	0.005	1.018	0.977
Ti(IV)-2-8d	0.02	1.00	1.00	0.014	1.042	0.944

<sup>a</sup> Ti, Al and P contents, either in gel or in solid, are expressed considering that the sum of all three contents is equal to 2, in such a way that, with the values given in the table, the composition corresponds to the general formula  $Ti_xAl_yP_zO_4$ .

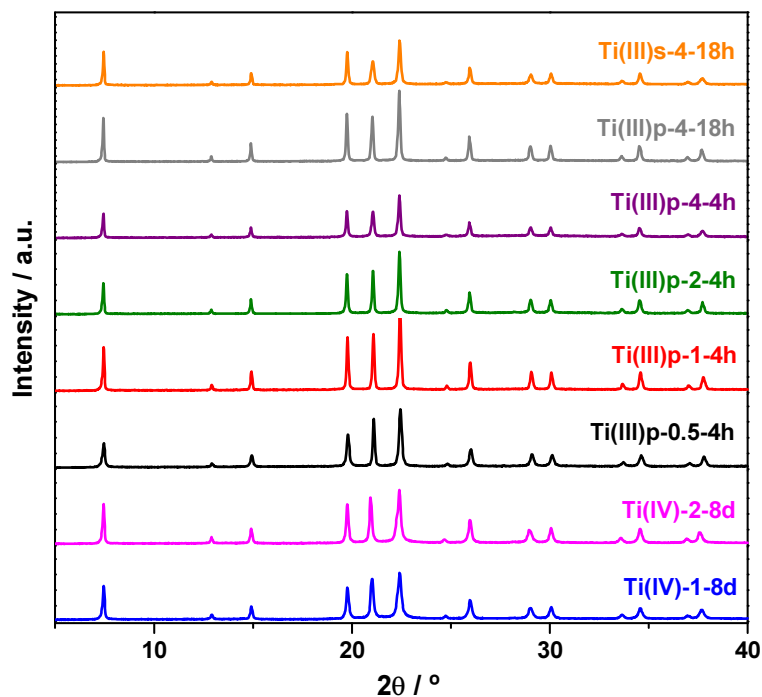


**Fig. 1.** PXRD patterns of the as-prepared TAPO-5 samples synthesized with different Ti(III) and Ti(IV) content.

Figure 2 shows the UV region of the diffuse reflectance UV-visible spectra of the calcined samples. It is worth recalling that titanium is in its 4+ oxidation state in all these samples, for Ti(III)APO-5 materials, which were purple-colored after the crystallization process [25, 26], became white due to the oxidation of Ti(III) to Ti(IV) during the drying process under ambient atmosphere or with the subsequent calcination process. The most intense band in the spectra (found at 205-232 nm) corresponds to charge-transfer transition between oxygen and tetrahedrally coordinated isolated titanium. Its maximum is red shifted when titanium loading increases. In the spectra of samples with lower content of the heteroatom, the maxima are found at a particularly low wavelength (205 nm). That position is unlike in conventional TAPO-5, particularly if they are calcined, and it is typical of Al-free Ti-zeolites [18]. For a similar titanium

content, the maxima of this band is red-shifted in the spectra of the Ti(IV)APO-5 samples with respect to these of the Ti(III)APO-5 samples: from 205 nm in Ti(III)p-0.5-4h to 215 nm in Ti(IV)-1-8d and from 215 nm in Ti(III)p-1-4h to 233 nm in Ti(IV)-2-8d. This systematic shift infers that titanium atoms have a different local coordination environment when the TAPO-5 is synthesized using a Ti(III) source [25, 26] instead of the Ti(IV) one. Additionally, the UV-visible spectra of all the samples present a contribution centered at *ca.* 280 nm, which is more pronounced in the spectra of samples with higher titanium content, these prepared at longer crystallization times and the Ti(IV)APO-5 ones. It can be noticed that the crystallization time seems to have a specific effect on the UV spectra. The two samples synthesized with the largest amount of Ti(III) in the gel have practically the same Ti content in the solids but the contribution at *ca.* 280 nm is much more pronounced in the sample synthesized at 18 h. The nature of this contribution, traditionally attributed to extraframework TiO<sub>2</sub>-containing species, has been recently assigned to Ti-O-Ti bond within the framework [20, 21]. These species are anyway undesired in Ti-zeolites from the point of view of catalytic activity, the isolated titanium centers being preferred [31].

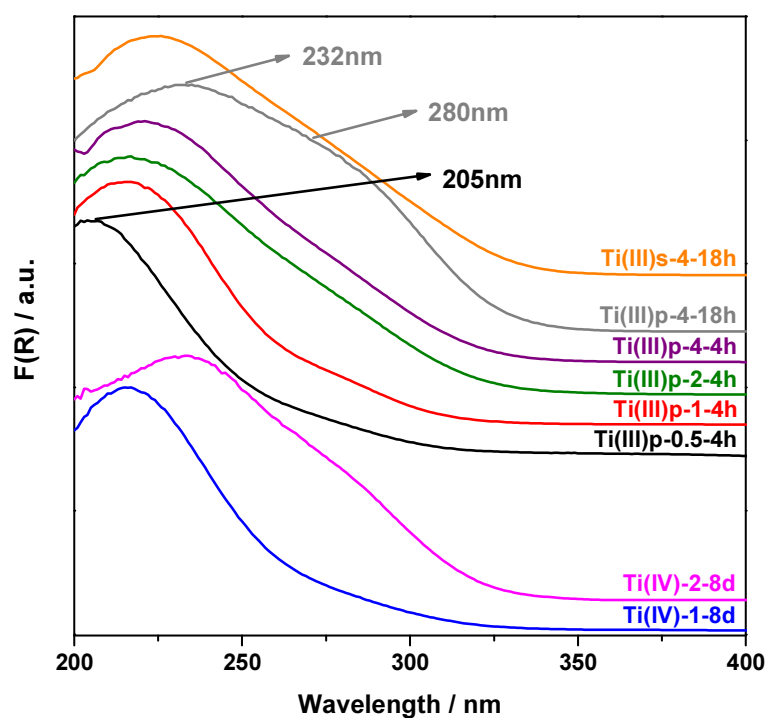


**Fig. 2.** UV region of the DRUV-visible spectra of the calcined samples Ti(III)APO-5 and Ti(IV)APO-5 with different titanium content.

SEM micrographs (Figure 3) show that the materials having the three lowest titanium contents, Ti(III)p-0.5-4h, Ti(III)p-1-4h and Ti(III)p-2-4h, are obtained as polycrystalline spherical-shape aggregates of elongated rod-like crystals. This morphology has been already observed in other MeAPO-5 materials prepared with the same SDA [32]. The particles of the samples with the highest titanium content synthesized with both  $\text{TiCl}_3$  sources (powder and in an aqueous solution of hydrochloric acid) are of hexagonal prism-like shape and formed by non-isolable fused crystals. The range of the aggregates sizes is from 10 to 30  $\mu\text{m}$  for these samples and are comparable to those of conventional catalysts synthesized with the Ti(IV) source, which also consist of aggregates of *ca.* 20 $\mu\text{m}$ .

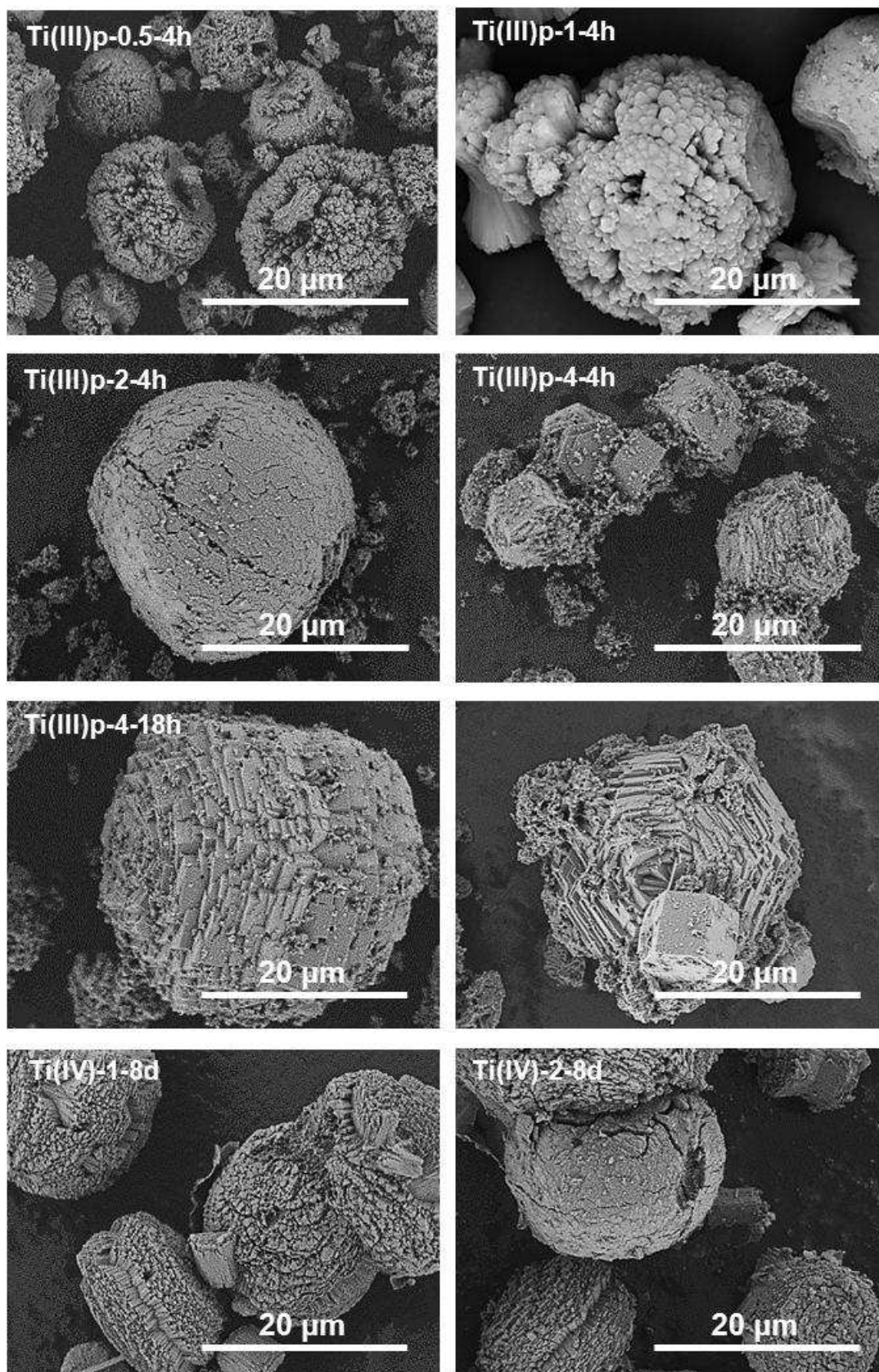


**Fig. 3.** Scanning electron micrographs of Ti(III)APO-5 and Ti(IV)APO-5 samples with different Ti content.

Textural properties of the calcined samples were studied by N<sub>2</sub> adsorption/desorption at 77 K. BET surface areas and micropore volumes estimated by the t-plot method are collected in Table 2. The sample Ti(III)p-4-4h has specific surface area and micropore volume lower than the values reported for conventional Ti(IV)APO-5 materials [10]. The comparison with its homologue crystallized during 18 h suggests that this is likely due to an uncompleted crystallization as it was also reflected in the XRD patterns (Figure 1).

**Table 2**

Specific surface areas and micropore volumes of Ti(III)APO-5 samples estimated from N<sub>2</sub> adsorption/desorption isotherms.

Sample	S <sub>BET</sub> (m <sup>2</sup> g <sup>-1</sup> )	Micropore volume (cm <sup>3</sup> g <sup>-1</sup> )
Ti(III)p-0.5-4h	336	0.115
Ti(III)p-1-4h	317	0.111
Ti(III)p-2-4h	245	0.083
Ti(III)p-4-4h	207	0.065
Ti(III)p-4-18h	302	0.112
Ti(III)s-4-18h	285	0.091
Ti(IV)APO-5	305	0.116

### 3.2. Effect of the Ti(III) source on the catalytic activity

TAPO-5 catalysts were tested in the oxidation of cyclohexene with H<sub>2</sub>O<sub>2</sub> under anhydrous conditions as described in the experimental section. The catalytic tests were designed to adequate the reaction conditions to the hydrophilic nature of the TAPO catalysts [27]. In our previous work, both conversion and selectivity of the sample here denoted as Ti(III)s-4-18h were compared to those of the conventional Ti(IV)APO-5 and a large-pore Ti-beta zeolite. This current work explores the catalytic activity of different

Ti(III)APO-5 catalysts prepared with different Ti content and different Ti(III) sources. Ti(III)APO-5 catalysts synthesized under identical crystallization conditions but with different Ti(III) sources, that is Ti(III)s-4-18h and Ti(III)p-4-18h, showed very different activity (Figure 4), the latter being more active. According to either traditional [33, 34] or recent [20-22] interpretation given to the contribution at 280 nm in the DRUV spectra (Figure 2), and assuming that Ti centers forming part of Ti-O-Ti bonds possess lower catalytic activity [31], the relative catalytic activity of those two samples was unexpected. The explanation to this apparent anomaly between catalytic behavior and spectroscopic features should be based on the singularities introduced by Ti(III) incorporation into the  $\text{AlPO}_4$  framework with respect to Ti(IV) [26].

Moreover, it must be noted that the only difference between both samples is the nature of the used  $\text{TiCl}_3$  source. The  $\text{TiCl}_3$  aqueous solution has a high and variable concentration of HCl which differs in the range of 20-30 wt. % from one commercial batch to another, making difficult to control certain synthesis conditions such as  $\text{Cl}^-$  concentration or pH, which can affect the subsequent crystallization process. Despite the relatively long crystallization time used to obtain the sample Ti(III)s-4-18h, the lack of control over the synthesis conditions could affect its crystallinity and its textural properties. As shown in Table 2, its micropore volume is below the typical value of conventional Ti(IV)APO-5 [10]. In other words, the use of solid  $\text{TiCl}_3$  is recommended instead of  $\text{TiCl}_3$  stabilized in HCl aqueous solution, as the former does not introduce any extra species in the gel, does not need to alter the general gel composition to compensate/control the starting pH and, maybe as a consequence of the two previous reasons, generates materials in a much more reproducible way.

On the other hand, the crystallization time also has an effect on the subsequent catalytic behavior. There is a significant difference in the conversion given by samples prepared

with the same Ti(III) source but crystallized for 4 h (Ti(III)p-4-4h) and 18 h (Ti(III)p-4-18h). Since this cannot be attributed to different titanium content or to an important effect of crystal size, the lower catalytic activity of the sample Ti(III)p-4-4h should be due to its lower crystallinity (Table 2 and Figure 1). Considering UV-visible spectra (Figure 2), again one would expect just the opposite result according to the intensity of the band at *ca.* 280 nm, which is higher for the sample crystallized for 18 h. Therefore, the low crystallinity and accordingly low surface area and micropore volume of sample Ti(III)p-4-4h (Table 2) seem to have a more important effect on the overall activity than the higher content of the more active isolated Ti species suggested by the UV-visible spectra. In any case, the fact that samples of high crystallinity are more active than similar ones with lower crystallinity indicates that, whatever is the role of the Ti(III)APO-5 catalysts in the general mechanism of the reaction, the catalytically-active part of the sample is the crystalline one.

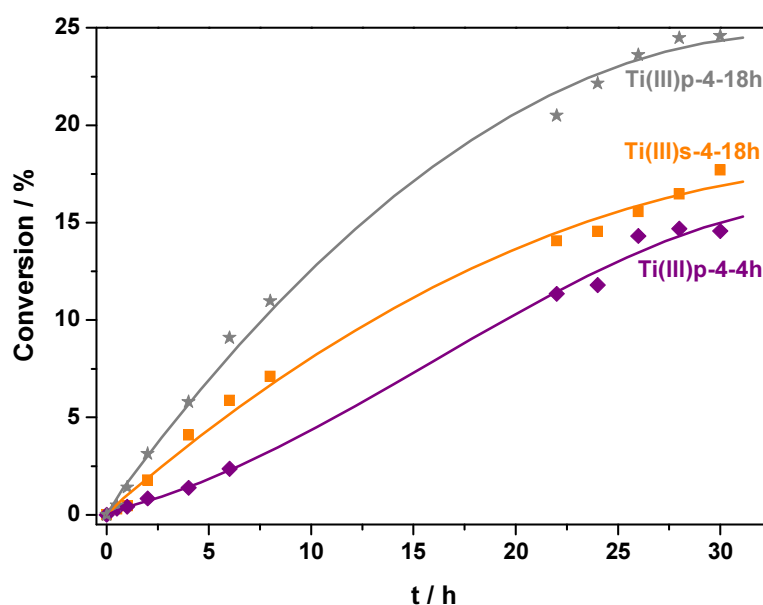


**Fig. 4.** Cyclohexene conversion over TAPO-5 catalysts prepared with different Ti(III) sources: Ti(III)s-4-18h (squares), prepared with aqueous hydrochloric acid solution of



TiCl<sub>3</sub>, and Ti(III)p-4-4h (diamonds) and Ti(III)p-4-18h (stars) prepared with TiCl<sub>3</sub> powder.

### 3.3. Effect of the Ti(III) content on the catalytic activity

The catalytic activity of the Ti(III)APO-5 samples with different titanium content has been also studied in the oxidation of cyclohexene with H<sub>2</sub>O<sub>2</sub> under anhydrous conditions. Figure 5 shows the cyclohexene conversion with the reaction time over different TAPO-5 catalysts prepared from TiCl<sub>3</sub> powder. The samples with the two lowest titanium contents, Ti(III)p-0.5-4h and Ti(III)p-1-4h, together with the sample Ti(III)p-4-18h, gave the highest conversions of the olefin. However, their titanium content is quite different, so the intrinsic activity per Ti center, that is, the turnover number (TON), is markedly different (Figure 6A and 6B). After 6 h of reaction, an inverse correlation, with almost exponential decay, between the turnover numbers and the titanium content in the Ti(III)APO-5 samples (full squares in Figure 6A) is observed. This result is in good agreement with the UV spectra of this series of samples as regards the shift to higher wavelength of the maximum of the charge transfer band and the increase of the contribution of the signal at *ca.* 280 nm, probably due to the presence of Ti-O-Ti pairs [20-22]. Taking these aspects into account, it can be inferred that a lower titanium content produces higher proportion of isolated titanium centers in the material, with a singular environment within the framework that makes them very active in the cyclohexene oxidation reaction.

After 24 h of reaction, the pattern of TON evolution with the titanium content (Figure 6B) is similar to that found after 6 h of reaction (Figure 6A), although, obviously, absolute values of TON increased from 6 h to 24 h. The comparison of catalytic activity per Ti center of the Ti-richest Ti(III)APO-5 samples shows that TON values are

substantially affected by the crystallization time, resulting the sample prepared at shorter time (and not fully crystallized) with lower TON values, as expected from the discussion of the previous section.

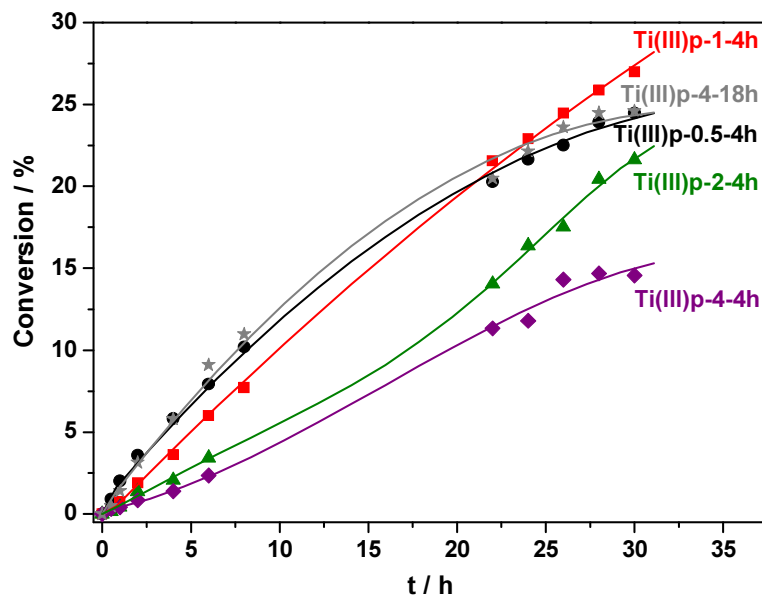


**Fig. 5.** Cyclohexene conversion over Ti(III)APO-5 catalysts prepared with  $\text{TiCl}_3$  powder and different titanium content: Ti(III)p-0.5-4h (circles), Ti(III)p-1-4h (squares), Ti(III)p-2-4h (triangles), Ti(III)p-4-4h (diamonds) and Ti(III)p-4-18h (stars).

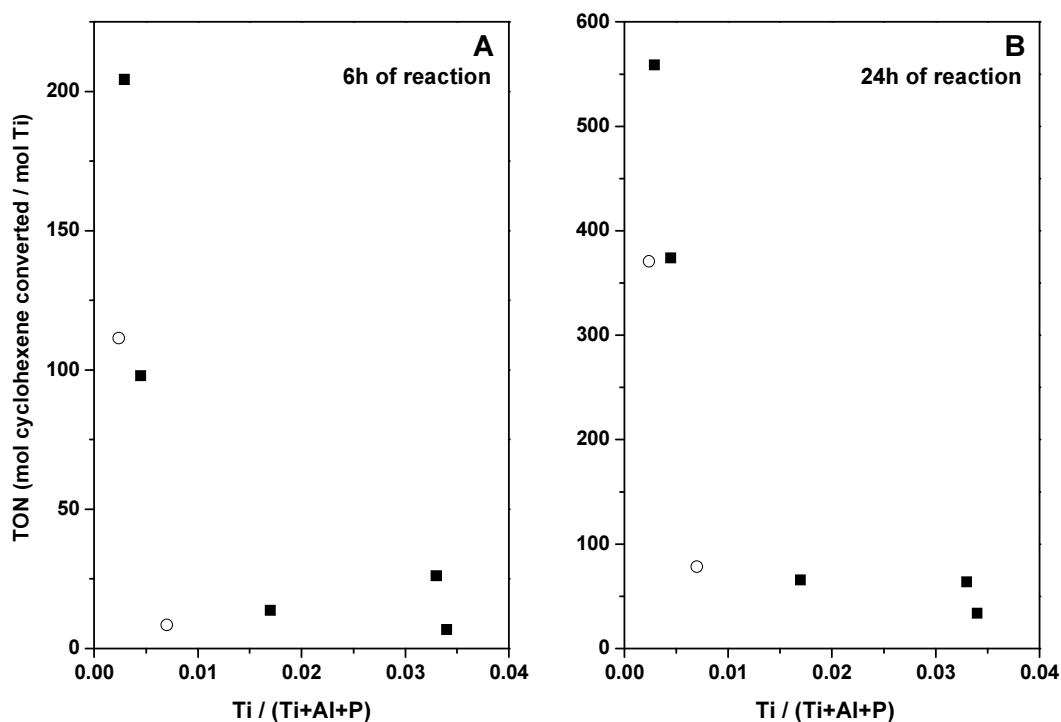


**Fig. 6.** Cyclohexene conversion per Ti center (TON) in Ti(III)APO-5 (full squares) and Ti(IV)APO-5 (open circles) samples with different titanium content after 6 h (A) and 24 h (B) of reaction.

Cyclohexene oxidation can take place through two different mechanisms [27, 35-38]: (i) a homolytic one involving radical species, and (ii) an heterolytic mechanism implying the oxidation of the double bond to give the epoxide as either final product or intermediate of different products formed by epoxide ring aperture. It is well-known [19, 31] that the latter mechanism is directed by Ti-zeolite catalysts while, on the contrary, the studied TAPO-5 materials mainly induced the reaction through the radical mechanism under anhydrous conditions [27]. All tested catalysts certify the preference of TAPO-5 to favor the reaction through the radical pathway, mostly leading to the allylic oxidation products, instead of those formed through the epoxidation of the

double bond. Table 3 summarizes the total conversion results, the yields corresponding to both reaction mechanisms and the product selectivity obtained for the Ti(III)APO-5 materials at the end of the reaction, after 30 h. Selectivity to the reaction products are quite similar for all catalysts, the most abundant product being 2-cyclohexenyl hydroperoxide [27] in all cases. Other side-products such as 2-cyclohexen-1-ol and 2-cyclohexen-1-one are also detected, surely coming from the hydroperoxide [39, 40]. Cyclohexanol and sometimes 1,2-cyclohexanediol, formed from the epoxide, are also detected at limited or negligible extension. These results could make Ti(III)APO-5 materials to become potential catalysts for certain applications that require the activation of the allylic position without affecting the double bond.

**Table 3**

Conversion and product selectivity in the oxidation of cyclohexene with H<sub>2</sub>O<sub>2</sub> under anhydrous conditions over Ti(III)APO-5 catalysts after 30 h of reaction.

Sample	Total conversion <sup>a</sup> /%	Yield <sup>b</sup> /%		Product selectivity <sup>c</sup> /%					
		Epoxidation	Radical	Epox	Chol	Diol	Enol	Enone	Chhp
Ti(III)p-0.5-4h	24	4	20	14	2	1	3	5	75
Ti(III)p-1-4h	27	4	23	12	2	-	3	8	75
Ti(III)p-2-4h	22	3	19	12	2	-	5	11	70
Ti(III)p-4-4h	15	4	11	14	7	3	7	12	57
Ti(III)p-4-18h	24	2	22	8	2	-	3	6	81
Ti(IV)-1-8d	16	4	12	21	5	-	3	2	69
Ti(IV)-2-8d	12	2	10	18	1	-	1	4	76

<sup>a</sup> Conversion calculated by the total addition of the yields of the resultant products.

<sup>b</sup> Sum of the yields of the products obtained through every mechanism.

<sup>c</sup> Epox, cyclohexene oxide; Chol, cyclohexanol; Diol, 1,2-cyclohexanediol; Enol, 2-cyclohexen-1-ol; Enone, 2-cyclohexen-1-one; Chhp, 2-cyclohexenyl hydroperoxide.

### 3.4. Influence of oxidation state of Ti source on the catalytic activity of TAPO-5.

This section focuses on a more extended comparison of the catalytic behavior of Ti(III)APO-5 and Ti(IV)APO-5 materials with different titanium content. The cyclohexene conversion levels reached by samples Ti(III)p-0.5-4h and Ti(III)p-1-4h are compared with those of Ti(IV)-1-8d and Ti(IV)-2-8d in Figure 7. Regardless the titanium content, Ti(III)APO-5 catalysts (full symbols) are always more active than the conventional Ti(IV)APO-5 (open symbols), at any tested reaction time.

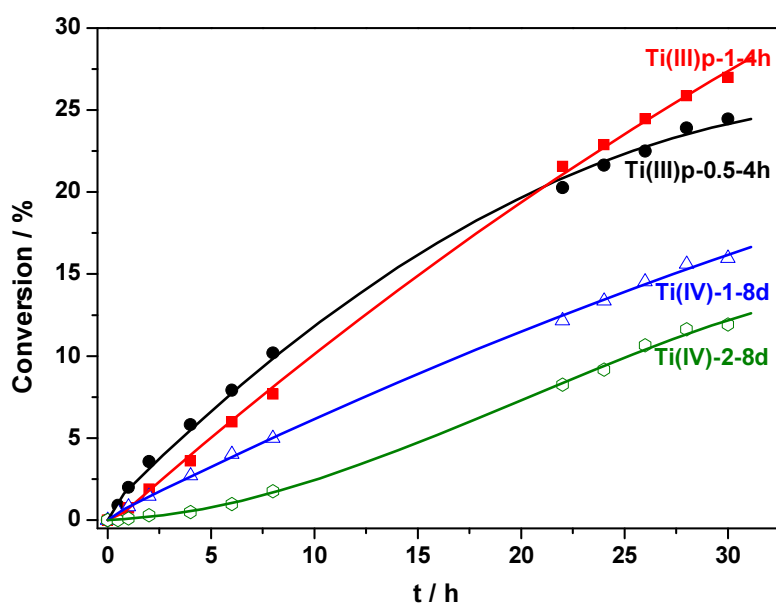


**Fig. 7.** Cyclohexene conversion catalyzed by Ti(III)APO-5 samples: Ti(III)p-0.5-4h (full circles) and Ti(III)p-1-4h (full squares), and Ti(IV)APO-5 materials: Ti(IV)-1-8d (open triangles) and Ti(IV)-2-8d (open hexagons).

On the other hand, the catalytic activity per titanium center is systematically much higher for the materials Ti(III)APO-5 at any time of reaction (Figure 6). On the contrary, no significant differences in the selectivities to the different reaction products were observed (Table 3). Thus, the most abundant product obtained with Ti(III)APO-5 materials, 2-cyclohexenyl hydroperoxide, is also the one with the highest selectivity for Ti(IV)APO-5 catalysts.

Although Table 3 breaks down the conversion into the selectivity to different products for different TAPO-5 catalysts after 30 h of reaction, a valid comparison of selectivity between different samples strictly requires referring it to the same conversion rather than the same reaction time. However, the here addressed reaction is very unusual in this sense, as two different reaction mechanisms coexist and they are taking place almost in consecutive sequence rather than in parallel. It means that imposing the condition of equal conversion level for selectivity comparison purposes could not be the best solution in this particular case, if it implies to compare very different reaction times. Consequently, we compare in Figure 8 the conversion and selectivity (to the sum of products formed by one or the other mechanism) along the reaction time, for the Ti(III)APO-5 and Ti(IV)APO-5 materials with the lowest and similar Ti content, instead of comparing the selectivities at a given similar conversion. The samples with the lowest Ti content were selected due to the exceptionally high TON values given by Ti(III)p-0.5-4h (Figure 6), which is likely due to the higher proportion of Ti occupying Al sites in the  $\text{AlPO}_4$  framework in this sample. Apart from the already commented higher conversion of the Ti(III)APO-5 sample, both catalysts have similar behavior in terms of selectivity. Thus, at long reaction times, in both cases the radical mechanism ends up dominating over the epoxidation one, which is however competing with the former at short times. It means that the selectivity to products formed via the radical mechanism (mainly 2-cyclohexenyl hydroperoxide, Table 3) simply increases by prolonging the reaction time. That strategy is based on the different kinetic trend of both mechanisms, since the epoxidation products yield curve is a kind of downward horizontal asymptote whereas that of the radical mechanism follows a linear tendency with time. Moreover, a detailed analysis of the difference in selectivity between both samples shows that, for this low Ti content, Ti(III)APO-5 is not only more active than

Ti(IV)APO-5 but it is also more selective to the radical path products (83 and 74 %, respectively, after 30 hours, Table 3), what makes Ti(III)APO-5 materials much more promising candidates as TAPO-based heterogeneous catalysts alternative to Ti-zeolites in the oxidation of cyclohexene with H<sub>2</sub>O<sub>2</sub> [27].

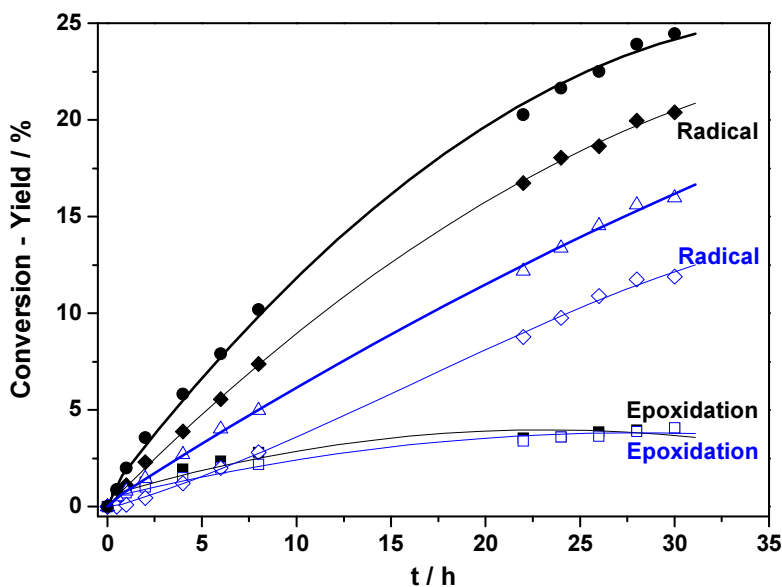


**Fig. 8.** Conversion (thick lines) and sum of the yield of products (thin lines) formed through radical (diamonds) and epoxidation (squares) mechanisms of the Ti-poorest Ti(III)APO-5 (full symbols) and Ti(IV)APO-5 (empty symbols) catalysts.

Given that the different catalytic activity shown by Ti(III)APO-5 and Ti(IV)APO-5 cannot be assigned to a drastic difference in crystal size (Figure 3), it could be attributed to the distinct mechanism of Ti incorporation imposed by the use of Ti sources with different titanium oxidation state. Some consequences of the different oxidation state of the titanium incorporated in the AlPO<sub>4</sub> framework were already noticed in the UV spectra (Figure 2). The spectra of calcined samples Ti(III)p-0.5-4h and Ti(III)p-1-4h presented narrower bands at lower wavelength and with a less intense contribution at 280 nm. All these catalytic and spectroscopic features of both Ti(III)APO-5 and

Ti(IV)APO-5 materials strongly evidence some differences in Ti environment, suggesting the presence of titanium centers with higher intrinsic activity in the material Ti(III)APO-5. Admitting that titanium occupying aluminum sites are the centers with the most relevant redox potential [20-22], the higher conversion of the samples Ti(III)APO-5 should imply a higher amount of titanium in that environment within the  $\text{AlPO}_4$  framework. In principle, that goal can be only achieved by the incorporation of the metal in a lower oxidation state, as Ti(III), in the synthesis gel.

In summary, the approach of incorporating Ti(III) instead of Ti(IV) ions into the  $\text{AlPO}_4$ -5 framework was successfully achieved, producing TAPO-5 catalysts of promising catalytic behavior. However, the exact nature of the Ti sites, as well as the relationship between the Ti environment and the catalytic activity, are far from being known.

Nevertheless, some insights based on different characterization techniques are given elsewhere [26].

## Conclusions

Ti(III)APO-5 materials have been successfully prepared using different Ti(III) sources, in a wide range of Ti content and after different crystallization times, using the AFI-specific structure directing agent  $\text{N,N}$ -methylcyclohexylamine (MCHA) and preparing the starting gel under inert atmosphere. At least part of Ti seems to be incorporated as Ti(III) into the  $\text{AlPO}_4$  framework. Although this Ti(III) is oxidized to Ti(IV) as soon as the sample is dried under ambient atmosphere, the aim of rerouting the conventional Ti incorporation in P sites of an  $\text{AlPO}_4$  framework towards its incorporation in Al sites has been somehow successful, producing TAPO-5 materials with unprecedented catalytic activity under the tested conditions. Thus, Ti(III)APO-5 materials resulted significantly



more active in the oxidation of cyclohexene with  $\text{H}_2\text{O}_2$  under anhydrous conditions than conventional Ti(IV)APO-5 ones. Moreover, very high activity per Ti center was achieved when Ti(III)APO-5 catalysts with low Ti content were used. Furthermore, these catalysts favor the oxidation of cyclohexene through the allylic position of the double bond, unlike Ti-containing silica-based nanoporous materials that favor the oxidation of cyclohexene through double bond epoxidation. Thinking in possible industrial applications, interestingly Ti(III)APO-5 catalysts are quite selective (even above 80 %) to 2-cyclohexenyl hydroperoxide, which can easily further react to give some oxidized cyclohexene derivatives having intact the double bond. Practically the same selectivity is also given by the less-active Ti(IV)APO-5 catalyst, which suggests that only Ti atoms surrounded by P (presumably abundant in Ti(III)APO-5 and scarce in Ti(IV)APO-5) are the catalytically-active centers.

### **Acknowledgments**

The authors thank Beatriz Bernardo-Maestro and Rubén Sepúlveda for their contributions in the preparation of the materials. They also acknowledge the Spanish Government for financial support (Projects MAT-2009-13569 and MAT-2012-31127). A. Alfayate acknowledges CSIC for a PhD Jae-Predoc fellowship.

## References

- [1] M. Taramasso, G. Perego, B. Notari, U.S. Patent 4,410,501 (1983).
- [2] P. Ratnasamy, D. Srinivas, H. Knözinger, *Adv. Catal.* 48 (2004) 1-169.
- [3] B. Notari, *Adv. in Catal.* 41 (1996) 253-334.
- [4] A. Corma, M.A. Camblor, P. Esteve, A. Martínez, J. Pérez-Pariente, *J. Catal.* 145 (1994) 151-158.
- [5] J.C. van der Waal, M.S. Rigutto, H. van Bekkum, *Appl. Catal. A* 167 (1998) 331-342.
- [6] V. Hulea, F. Fajula, J. Bousquet, *J. Catal.* 198 (2001) 179-186.
- [7] V. Hulea, E. Dumitriu, *Appl. Catal. A* 277 (2004) 99-106.
- [8] T. Blasco, A. Corma, M.T. Navarro, J. Pérez-Pariente, *J. Catal.* 156 (1995) 65-74.
- [9] B.M.T. Lok, B.K. Marcus, E. Flanigen, U.S. Patent 4,500,651 (1985).
- [10] M.H. Zahedi-Niaki, P.N. Joshi, S. Kaliaguine, *Progress in zeolite and microporous materials*, in: S.K.I. Hakze Chon, U. Young Sun (Eds.), *Studies in Surface Science and Catalysis*, Elsevier, Seoul, 1997, Vol. 105, pp. 1013-1020.
- [11] F.J. Luna, S.E. Ukawa, M. Wallau, U. Schuchardt, *J. Mol. Catal. A: Chem.* 117 (1997) 405-411.
- [12] M. H. Zahedi-Niaki, M.P. Kapoor, S. Kaliaguine, *J. Catal.* 177 (1998) 231-239.
- [13] A. Tuel, *Zeolites* 15 (1995) 228-235.
- [14] S.O. Lee, R. Raja, K.D.M. Harris, J.M. Thomas, B.F.G. Johnson, G. Sankar, *Angew. Chem., Int. Ed.* 42 (2003) 1520-1523.
- [15] B.Y. Hsu, S. Cheng, J.M. Chen, *J. Mol. Catal. A: Chem.* 149 (1999) 7-23.
- [16] A. Corma, P. Esteve, A. Martínez, *J. Catal.* 161 (1996) 11-19.
- [17] J.C. van der Waal, H. van Bekkum, *J. Mol. Catal. A: Chem.* 124 (1997) 137-146.
- [18] T. Blasco, M.A. Camblor, A. Corma, P. Esteve, J.M. Guil, A. Martínez, J.A. Perdigón-Melón, S. Valencia, *J. Phys. Chem. B* 102 (1998) 75-88.
- [19] J.C. Torres, D. Cardoso, R. Pereira, *Microporous Mesoporous Mater.* 136 (2010) 97-105.
- [20] S. Maurelli, M. Vishnuvarthan, M. Chiesa, G. Berlier, S. Van Doorslaer, *J. Am. Chem. Soc.* 133 (2011) 7340-7343.
- [21] S. Maurelli, M. Vishnuvarthan, G. Berlier, M. Chiesa, *Phys. Chem. Chem. Phys.* 14 (2012) 987-995.
- [22] C. Novara, A. Alfayate, G. Berlier, S. Maurelli, M. Chiesa, *Phys. Chem. Chem. Phys.* 15 (2013) 11099-11105.
- [23] S. del Val, T. Blasco, E. Sastre, J. Pérez-Pariente, *J. Chem. Soc., Chem. Commun.* (1995) 731-732.
- [24] A. M. Prakash, S. Unnikrishnan, K.V. Rao, *Appl. Catal. A* 110 (1994) 1-10.
- [25] A. Alfayate, M. Sánchez-Sánchez, J. Pérez-Pariente, ES Patent PCT/ES2012/070436 (2011).
- [26] A. Alfayate, M. Sánchez-Sánchez, J. Pérez-Pariente, manuscript in preparation.
- [27] A. Alfayate, C. Márquez-Álvarez, M. Grande-Casas, B. Bernardo-Maestro, M. Sánchez-Sánchez, J. Pérez-Pariente, *Catal. Today* 213 (2013) 211-218.
- [28] M. Sánchez-Sánchez, G. Sankar, A. Simperler, R.G. Bell, C.R.A. Catlow, J.M. Thomas, *Catal. Lett.* 88 (2003) 163-167.
- [29] M. Sánchez-Sánchez, R. van Grieken, D.P. Serrano, J.A. Melero, *J. Mat. Chem.* 19 (2009) 6833-6841.
- [30] A.M. Prakash, L. Kevan, M.H. Zahedi-Niaki, S. Kaliaguine, *J. Phys. Chem. B*, 103 (1999) 831-837.
- [31] B. Notari, *Innovation in zeolite materials science*, P.J. Grobet, W.J. Mortier, E.F. Vansant, G. Schulz-Ekloff (Eds.) *Studies in Surface Science and Catalysis*, Elsevier, Belgium, 1988, Vol. 37, pp. 413-425.

- [32] A. Manjón-Sanz, M. Sánchez-Sánchez, P. Muñoz-Gómez, R. García, E. Sastre, *Microporous Mesoporous Mater.* 131 (2010) 331-341.
- [33] E. Gianotti, A. Frache, S. Coluccia, J.M. Thomas, T. Maschmeyer, L. Marchese, *J. Mol. Catal. A: Chem.* 204-205 (2003) 483-489.
- [34] S. Bordiga, S. Coluccia, C. Lamberti, L. Marchese, A. Zecchina, F. Boscherini, F. Buffa, F. Genoni, G. Leofanti, *J. Phys. Chem.* 98 (1994) 4125-4132.
- [35] R.R. Sever, R. Alcalá, J.A. Dumesic, T.W. Root, *Microporous Mesoporous Mater.* 66 (2003) 53-67.
- [36] J. Vernimmen, M. Guidotti, J. Silvestre-Albero, E.O. Jardim, M. Mertens, O.I. Lebedev, G. Van Tendeloo, R. Psaro, F. Rodriguez-Reinoso, V. Meynen, P. Cool, *Langmuir*, 27 (2011) 3618-3625.
- [37] E. Jorda, A. Tuel, R. Teissier, J. Kervennal, *J. Catal.* 175 (1998) 93-107.
- [38] J.M. Fraile, J.I. Garcia, J.A. Mayoral, E. Vispe, *J. Catal.* 204 (2001) 146-156.
- [39] S.M. Mahajani, M.M. Sharma, T. Sridhar, *Chem. Eng. Sci.* 54 (1999) 3967-3976.
- [40] H.E.B. Lempers, J.D. Chen, R.A. Sheldon, *Catalysis by microporous materials*, in: H.K. Beyer, H.G. Karge, I. Kiricsi, J.B. Nagy (Eds.), *Studies in Surface Science and Catalysis*, Elsevier, Hungary, 1995, Vol. 94, pp. 705-712.

## Captions

### Table 1

Ti, Al and P content of the gels and as-prepared Ti(III)APO-5 and Ti(IV)APO-5 samples determined by ICP-OES.

### Table 2

Specific surface areas and micropore volumes of Ti(III)APO-5 samples estimated from N<sub>2</sub> adsorption/ desorption isotherms.

### Table 3

Conversion and product selectivity in the oxidation of cyclohexene with H<sub>2</sub>O<sub>2</sub> under anhydrous conditions over Ti(III)APO-5 catalysts after 30 h of reaction.

**Fig. 1.** PXRD patterns of the as-prepared TAPO-5 samples synthesized with different Ti(III) and Ti(IV) content.

**Fig. 2.** UV region of the DRUV-visible spectra of the calcined samples Ti(III)APO-5 and Ti(IV)APO-5 with different titanium content.

**Fig. 3.** Scanning electron micrographs of Ti(III)APO-5 and Ti(IV)APO-5 samples with different Ti content.

**Fig. 4.** Cyclohexene conversion over TAPO-5 catalysts prepared with different Ti(III) sources: Ti(III)s-4-18h (squares), prepared with aqueous hydrochloric acid solution of

TiCl<sub>3</sub>, and Ti(III)p-4-4h (diamonds) and Ti(III)p-4-18h (stars) prepared with TiCl<sub>3</sub> powder.

**Fig. 5.** Cyclohexene conversion over Ti(III)APO-5 catalysts prepared with TiCl<sub>3</sub> powder and different titanium content: Ti(III)p-05-4h (circles), Ti(III)p-1-4h (squares), Ti(III)p-2-4h (triangles), Ti(III)p-4-4h (diamonds) and Ti(III)p-4-18h (stars).

**Fig. 6.** Cyclohexene conversion per Ti center (TON) in Ti(III)APO-5 (full squares) and Ti(IV)APO-5 (open circles) samples with different titanium content after 6 h (A) and 24 h (B) of reaction.

**Fig. 7.** Cyclohexene conversion catalyzed by Ti(III)APO-5 samples: Ti(III)p-05-4h (full circles) and Ti(III)p-1-4h (full squares), and Ti(IV)APO-5 materials: Ti(IV)-1-8d (open triangles) and Ti(IV)-2-8d (open hexagons).

**Fig. 8.** Conversion (thick lines) and sum of the yield of products (thin lines) formed through radical (diamonds) and epoxidation (squares) mechanisms of the Ti-poorest Ti(III)APO-5 (full symbols) and Ti(IV)APO-5 (empty symbols) samples.